

AD618023

# AIR FORCE INSTITUTE OF TECHNOLOGY



AIR UNIVERSITY  
UNITED STATES AIR FORCE

INTERFEROMETER STUDY  
OF NATURAL CONVECTION INSIDE A  
HORIZONTAL CYLINDRICAL CAVITY

THESIS

GAM 65A/ME/65-3 Richard Irwin Erb  
Captain USAF

45-2

copy of	HARD COPY	\$ 2.00
	MICROFICHE	\$ 0.50

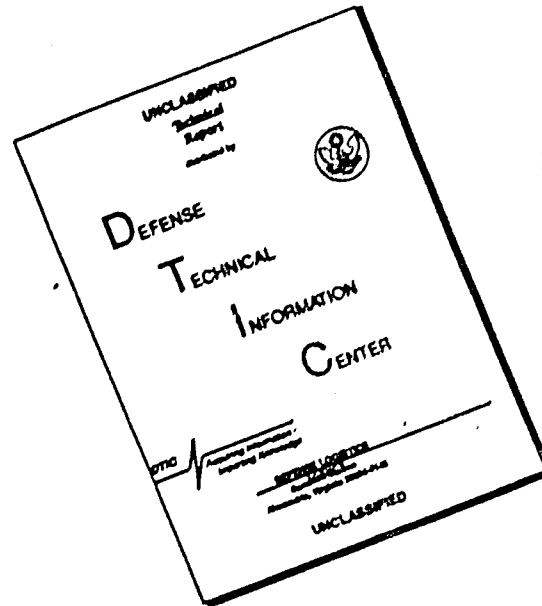
## SCHOOL OF ENGINEERING

WRIGHT-PATTERSON AIR FORCE BASE, OHIO

DDC  
JUL 26 1965  
ISIA D

ARCHIVE COPY

# DISCLAIMER NOTICE



THIS DOCUMENT IS BEST QUALITY AVAILABLE. THE COPY FURNISHED TO DTIC CONTAINED A SIGNIFICANT NUMBER OF PAGES WHICH DO NOT REPRODUCE LEGIBLY.

INTERFEROMETER STUDY OF NATURAL CONVECTION  
INSIDE A HORIZONTAL CYLINDRICAL CAVITY

THESIS

Presented to the Faculty of the School of Engineering of  
the Air Force Institute of Technology  
Air University  
in Partial Fulfillment of the  
Requirements for the Degree of  
Master of Science

by

Richard Irwin Erb, B.S.

Captain USAF

Graduate Aerospace-Mechanical Engineering

March 1965

### Preface

This investigation was conducted to provide experimental data on the transient heat transfer phenomena taking place within a horizontal cylindrical cavity with a non-uniform surface temperature distribution. The study was suggested by Mr. Erich E. Soehngen, Director, Thermomechanics Research Laboratory, Aerospace Research Laboratories.

I have attempted to present my findings in a manner understandable to a reader with a basic knowledge of heat transfer and of the interferometer.

I wish to acknowledge the guidance and suggestions received from Mr. Soehngen and from my faculty advisor, Dr. Andrew J. Shine, Head of the Mechanical Engineering Department.

Richard I. Erb

Contents

	Page
Preface . . . . .	ii
List of Figures . . . . .	iv
List of Symbols . . . . .	v
Abstract . . . . .	vi
I. Introduction . . . . .	1
II. Experimental Apparatus . . . . .	3
Test Cylinder . . . . .	3
Interferometer . . . . .	5
Temperature Recorder . . . . .	6
Cameras . . . . .	6
III. Procedure . . . . .	7
IV. Results . . . . .	9
Single-heater Configurations . . . . .	10
Multiple-heater Configurations . . . . .	17
V. Discussion of Results . . . . .	20
Single-heater Configurations . . . . .	20
Multiple-heater Configurations . . . . .	21
VI. Conclusions and Recommendations . . . . .	24
Bibliography . . . . .	26

List of Figures

Figure		Page
1	Fiberglass Cylinder . . . . .	3
2	Sketch of Fiberglass Cylinder . . . . .	4
3	Interferometer . . . . .	5
4	Sketch of Interferometer . . . . .	5
5	Location of Single Heaters . . . . .	9
6	Isotherm Patterns for Various Heater Locations after Five Minutes of Heating .	11
7	Variation of Local Heat Transfer Co- efficient with Time and Position . . .	12
8	Variation of Local $T_w$ with Time and Position . . . . .	13
9	Variation of Local $q_w$ with Time and Position . . . . .	13
10	Variation of Isotherms and Heat Trans- fer Coefficient with Time for a Single Heater Located at $\theta = 7.5$ degrees . . .	14
11	Variation of Isotherms and Heat Trans- fer Coefficient with Time for a Single Heater Located at $\theta = 112.5$ degrees . .	15
12	Variation of Heat Transfer from the Cylinder Wall in the Vicinity of a Single Heater Located at $\theta = 142.5$ degrees . . . . .	16
13	Isotherm Patterns for Multiple-Heater Configurations after Five Minutes of Heating . . . . .	18
14	Isotherm Patterns for Multiple-Heater Configurations after Five Minutes of Heating . . . . .	19

List of Symbols

Symbol	Quantity	Units
A	Area	ft <sup>2</sup>
e	Fringe number	
h	Local heat transfer coefficient at the cylinder wall adjacent to the center of the heating element	Btu/hr ft <sup>2</sup> F
k	Thermal conductivity	Btu/hr ft F
L	Length of test cylinder	ft
P	Pressure	lb/ft <sup>2</sup>
q	Heat transfer = $-k_w (dt/dr)_w$	Btu/hr ft <sup>2</sup>
R	Gas constant	ft lb <sub>f</sub> /lb <sub>m</sub> R
r	Distance measured inward along radials from the cylinder wall	ft
T	Temperature	F
t	Time	minutes
Y	Wave length of light	A
ρ	Density	lb/ft <sup>3</sup>
n	Index of refraction	
θ	Angle measured clockwise from the top of the cylinder	degrees

Subscripts

e	Fringe number
o	Standard condition
r	Reference condition
w	Condition at cylinder wall

Abstract

An optical interferometer was used to observe the isotherms which developed within a horizontal fiberglass cylinder as it was non-uniformly heated in axial strips to a maximum wall temperature of 200 F. It was found that when single strips were heated separately, the local heat transfer coefficients at the cylinder wall adjacent to each heater reached a maximum value in the region 20° to 25° below where the wall surface was vertical. Also, the magnitude of the coefficients increased with time for about the first six minutes of heating and then decreased slightly. Numerous photographs are included which show the isothermal patterns formed when various segments of the cylinder wall were heated.



INTERFEROMETER STUDY OF NATURAL CONVECTION  
INSIDE A HORIZONTAL CYLINDRICAL CAVITY

I. Introduction

Circulation by natural convection inside a cavity results from the action of body forces on the fluid. These forces are proportional to differences in fluid density within the cavity. When the inner surface of a cylinder is at the same temperature as the surrounding fluid, the body forces acting on the fluid are in equilibrium with the hydrostatic pressure and thus no flow occurs. However, if the cylinder is heated, a temperature gradient is established. As the heat is transferred from the wall to the surrounding fluid, the density of the fluid adjacent to the wall decreases producing an unbalanced force in the fluid. This unbalanced or buoyant force causes the fluid to be accelerated, with the particles near the wall moving most rapidly.

The heat transfer mechanism described above occurs in circular cylinders, such as storage fuel tanks or pressure bottles, when subjected to external heating under the influence of climatic conditions. Liquid fuel rockets subjected to aerodynamic heating and solar irradiation may under certain flight conditions be included in this consideration.

Much data is available on heat transfer by natural

convection along heated vertical surfaces. Less is known about this heat transfer from horizontal or from inclined (Ref 3) surfaces and even less for combinations of such surfaces, especially if these surfaces are curved.

The purpose of this study included two objectives. One objective was to qualitatively investigate the transient natural convective heat transfer phenomena occurring within a horizontal cylindrical cavity as the walls of the cylinder are heated. The other objective was to make an analysis of six single-heater configurations and to calculate the resulting transient local heat transfer coefficients.

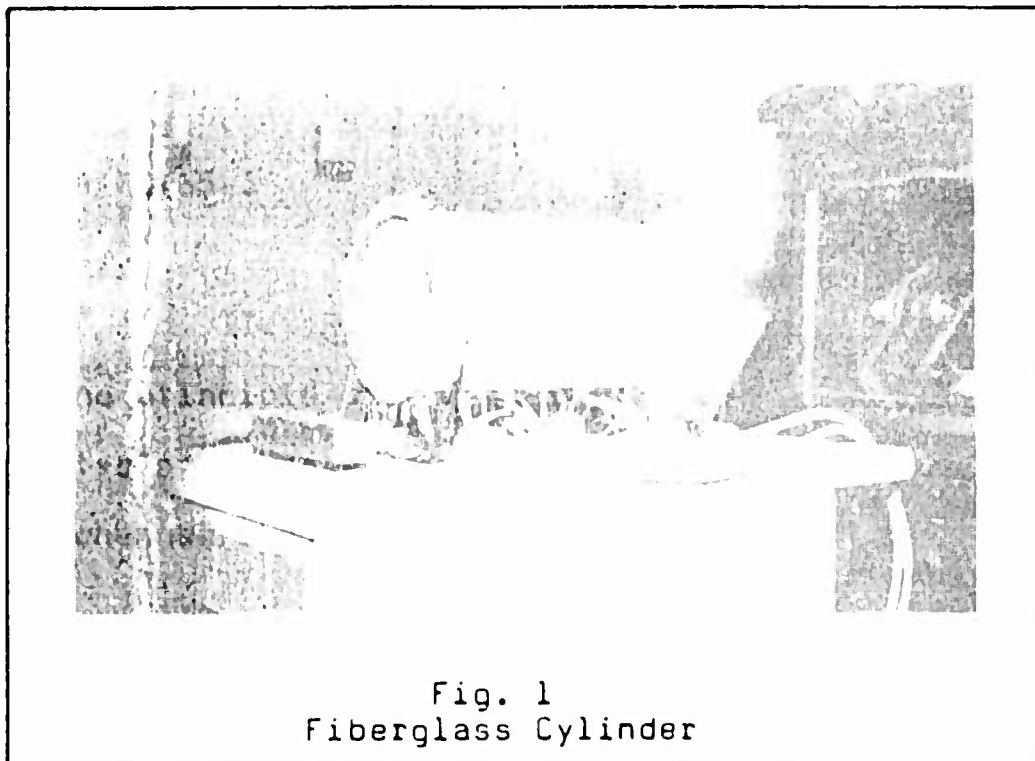
This experimental investigation was based on an interferometric study of a fiberglass cylinder which was five inches in diameter and one foot long. The cylinder, closed by glass windows at both ends and vented to the atmosphere, was non-uniformly heated in horizontal strips to a maximum wall temperature of 200 F. Because of this relatively low temperature, radiation and conduction effects were neglected.

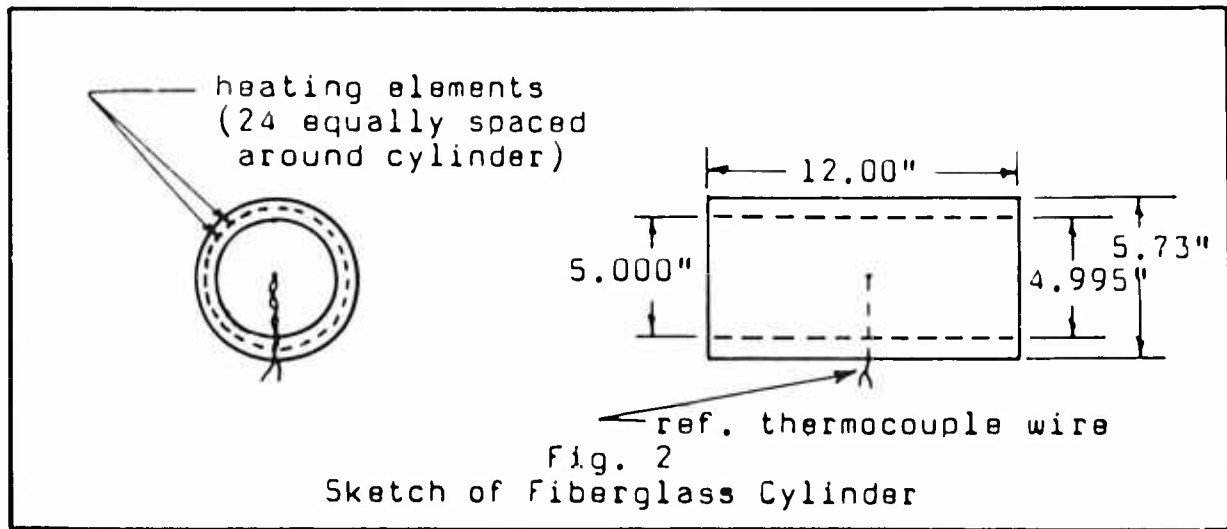
## II. Experimental Apparatus

The principle pieces of apparatus for this study consisted of a heated cylinder, an interferometer, a multi-channel recorder, and two cameras.

### Test Cylinder

The test subject, shown in Fig. 1, was a horizontally-suspended fiberglass cylinder which had 24 electric heating elements embedded in it lengthwise. Wall temperatures were measured by use of thermocouples placed between each of the heaters. A single thermocouple was suspended in the center of the cylinder as shown in Fig. 2 to provide a reference temperature measurement.



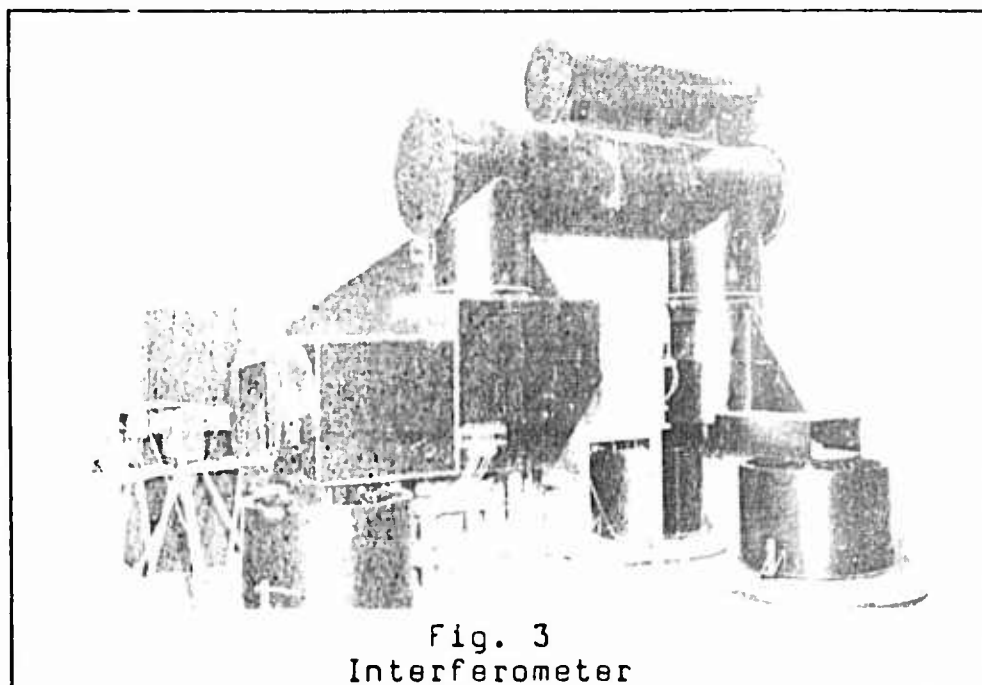


Interferometer-quality glass plates were placed at each end of the cylinder and were insulated from the cylinder walls by felt washers. The cylinder was supported by four adjustable screws topped with pointed phenolic caps to reduce heat transfer away from the cylinder. Small holes were drilled along the bottom of the cylinder to vent it to the atmosphere.

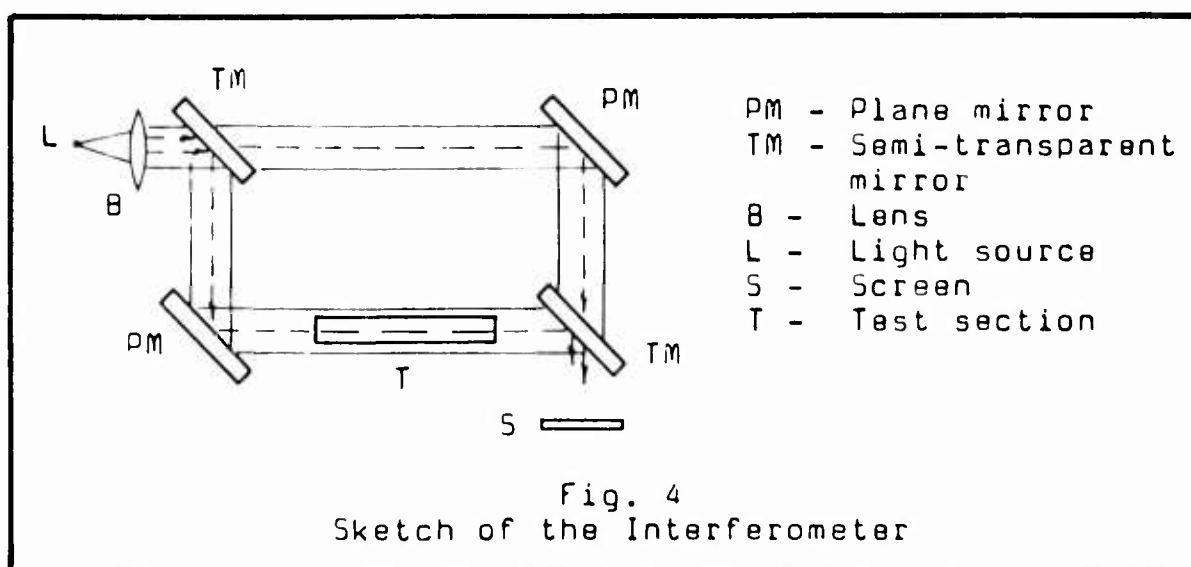
The heating elements were Nichrome ribbon with a resistance of 0.496 ohms per foot. Each element had a variable resistor connected across it. Electrical energy for the heating circuits was obtained from a DC power supply. When more than one heating element was used, the elements were connected in series.

### Interferometer

The optical interferometer used in this study is shown in Fig. 3. A mercury vapor light source was used



with a Wratten 77A filter to produce light with a wave length of 5461A. Mirrors in the interferometer were adjusted by small electric motors operated remotely from a control panel.



A sketch of the optical path of an interferometer is shown in Fig. 4. Details of operation may be found in Ref 2.

#### Temperature Recorder

The 25 thermocouples were connected to a terminal strip from which any 16 could then be connected to a multi-channel recorder which was modified to obtain maximum accuracy in the temperature range of 60 to 220 F. Each of the 16 temperature readings were recorded once every minute during tests.

#### Cameras

An electrically operated 70mm camera, equipped with a clock and data chamber, was used to take interferograms at a rate varying from one frame per second to one frame per two minutes. Dupont Superior 4 film was used with an exposure time of 1/50th of a second.

A Michell 16mm movie camera was used to make a fourteen minute moving picture of the thermal pattern development for various heater configurations. Ektachrome commercial film was used with a shutter speed of 1/72 seconds.

### III. Procedure

Each run was begun with the cylinder and its contents at the room temperature. Then, depending on the heater configuration to be studied, power at the rate of 7.3 watts was applied to each heater. This rate of heating was selected because it resulted in good fringe definition and still allowed adequate time for recording data. Interferograms of the heating process were taken at 0.5, 3.5, 6.5, 9.5, and approximately 30 minutes. The temperatures about the cylinder wall and the reference temperature at the center of the cylinder were continuously recorded.

For configurations where heat transfer coefficients were calculated, Kodalith positive contact prints were made to avoid paper distortion and to improve fringe definition. Measurements of fringe spacing were made on these prints along radials drawn to a point on the cylinder wall adjacent to the middle of each heating element. Then the heat transfer coefficients were determined by the following method. A reference density  $\rho_r$  was calculated using room barometric pressure and the reference temperature in the center of the cylindrical cavity. The density at each fringe was found using equation (1) which was developed by Eckert and Soehngen (Ref 2:2-3).

$$\rho_e = \rho_r - \left( \frac{\rho_o \gamma_o}{n_o - 1} \right) \frac{1}{L} e \quad (1)$$

Then the temperature distribution in the flow field was calculated using the perfect gas law, equation (2), assuming that pressure remained constant over the field.

$$T_g = \frac{P_r}{\rho_g R} \quad (2)$$

Heat transfer coefficients were obtained by using the following standard heat transfer equations found in Ref 2.

$$q = hA (T_w - T_r) \quad (3)$$

$$q = -k_w A \left( \frac{dT}{dr} \right)_w \quad (4)$$

Equating equations (3) and (4) and solving for h, the local heat transfer coefficient was expressed as

$$h = \frac{-k_w \left( \frac{dT}{dr} \right)_w}{T_w - T_r} \quad (5)$$

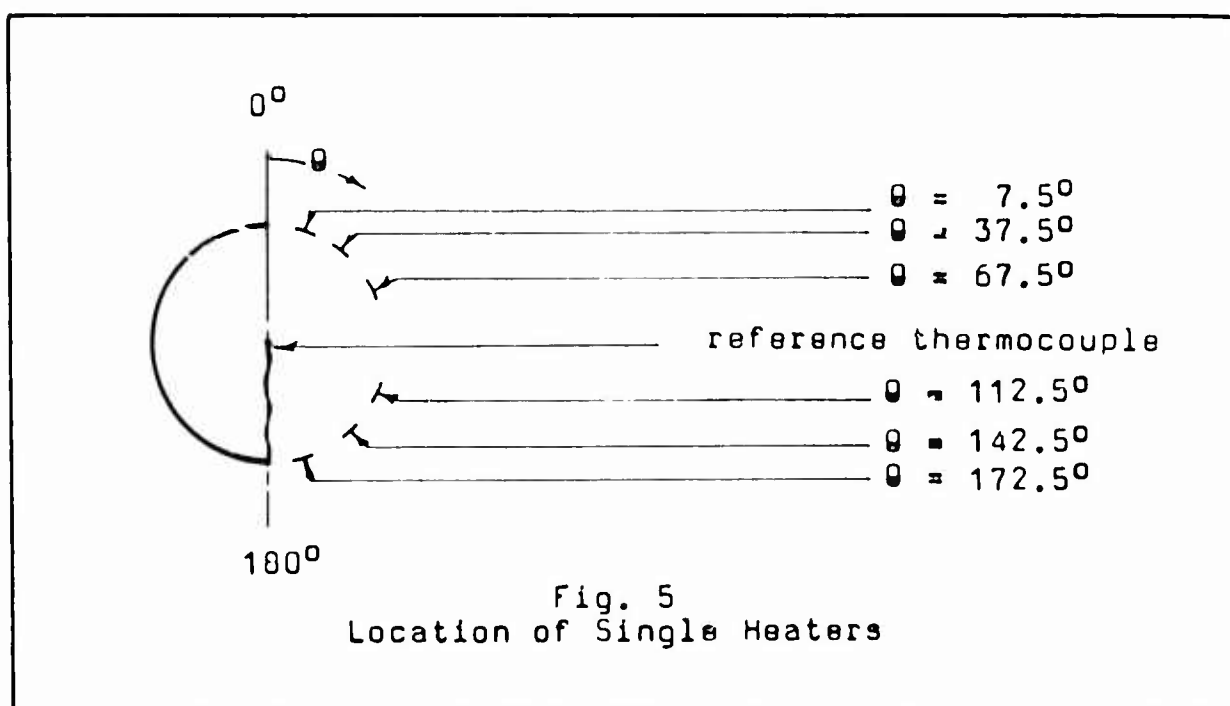
The temperature gradient at the wall  $\left( \frac{dT}{dr} \right)_w$  and the wall temperature  $T_w$  were obtained from a plot of  $T_g$  vs  $r$ , where the location of the fringes  $r$  was measured on a photograph of the interference pattern. Values of  $k_w$  were found in Ref 1:504.



#### IV. Results

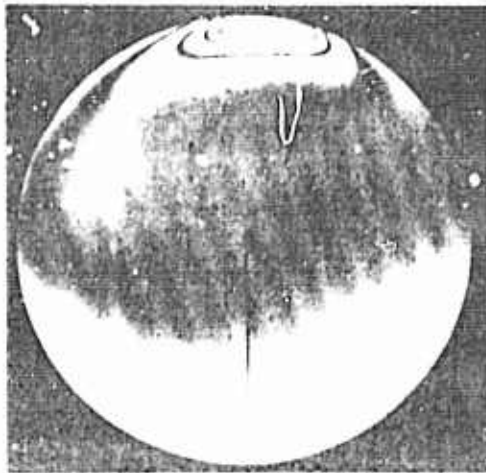
Numerous pictures are included as results because one of the primary objectives of this study was to qualitatively investigate the heat transfer phenomena taking place within the cylinder.

Heat transfer coefficients were calculated for six single-heater configurations. The location of these heaters is shown in Fig. 5.

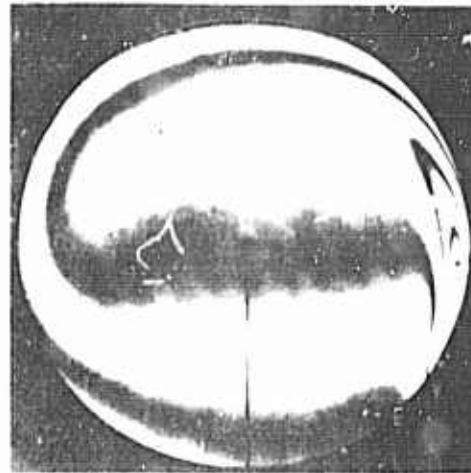


### Single-Heater Configurations

Photographs of the isotherms formed at each heater element after five minutes of heating are shown in Fig. 6. In Fig. 7 are shown the results of this study in the form of the heat transfer coefficient at a point on the wall at the heater as a function of heater position and time; and Figures 8 and 9 show the corresponding values of  $T_w$  and  $q_w$ . Figures 10 and 11 show typical interferograms which were used to determine the information for all curves. Fig. 12 shows the variation of heat transfer coefficients over the cylinder wall in the vicinity of the heater located at  $\theta = 142.5^\circ$ .



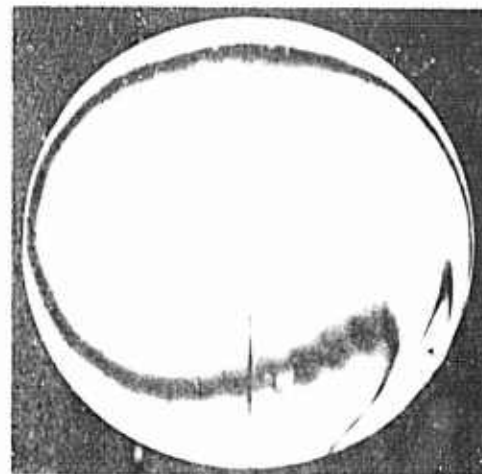
$$\theta = 7\frac{1}{2}^{\circ}$$



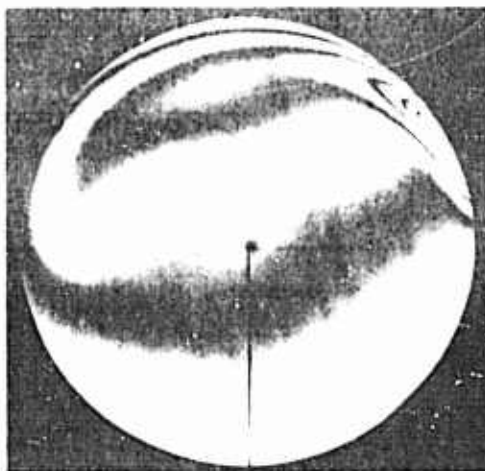
$$\theta = 112\frac{1}{2}^{\circ}$$



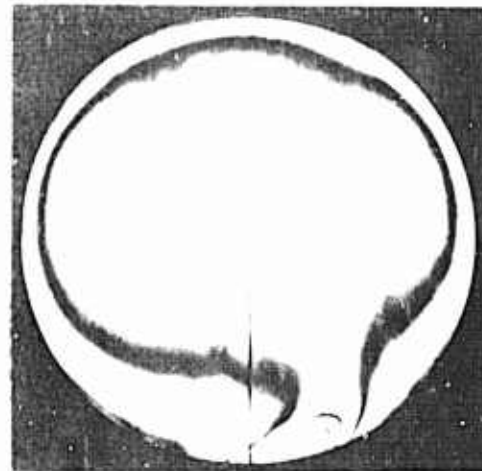
$$\theta = 37\frac{1}{2}^{\circ}$$



$$\theta = 142\frac{1}{2}^{\circ}$$

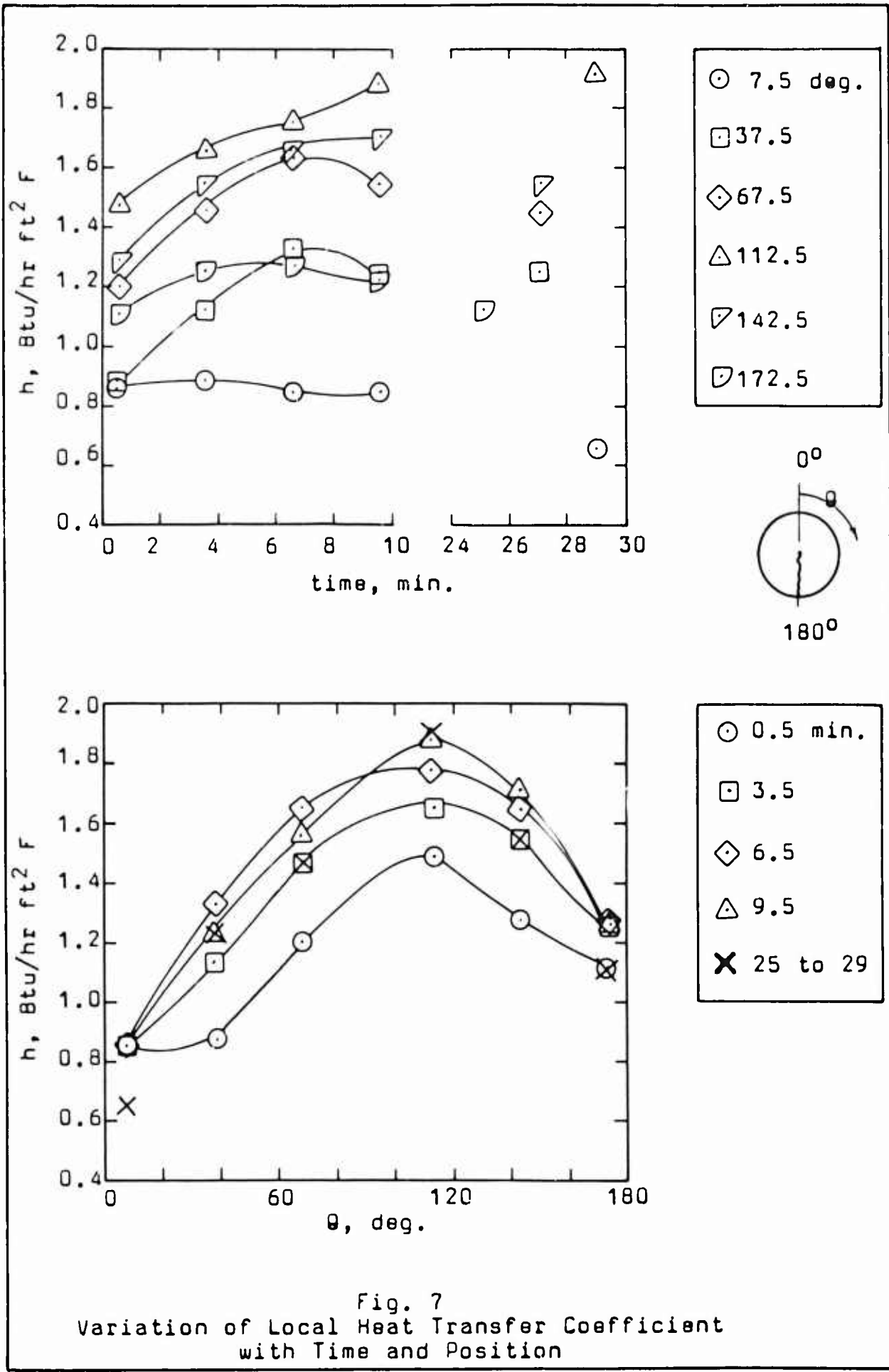


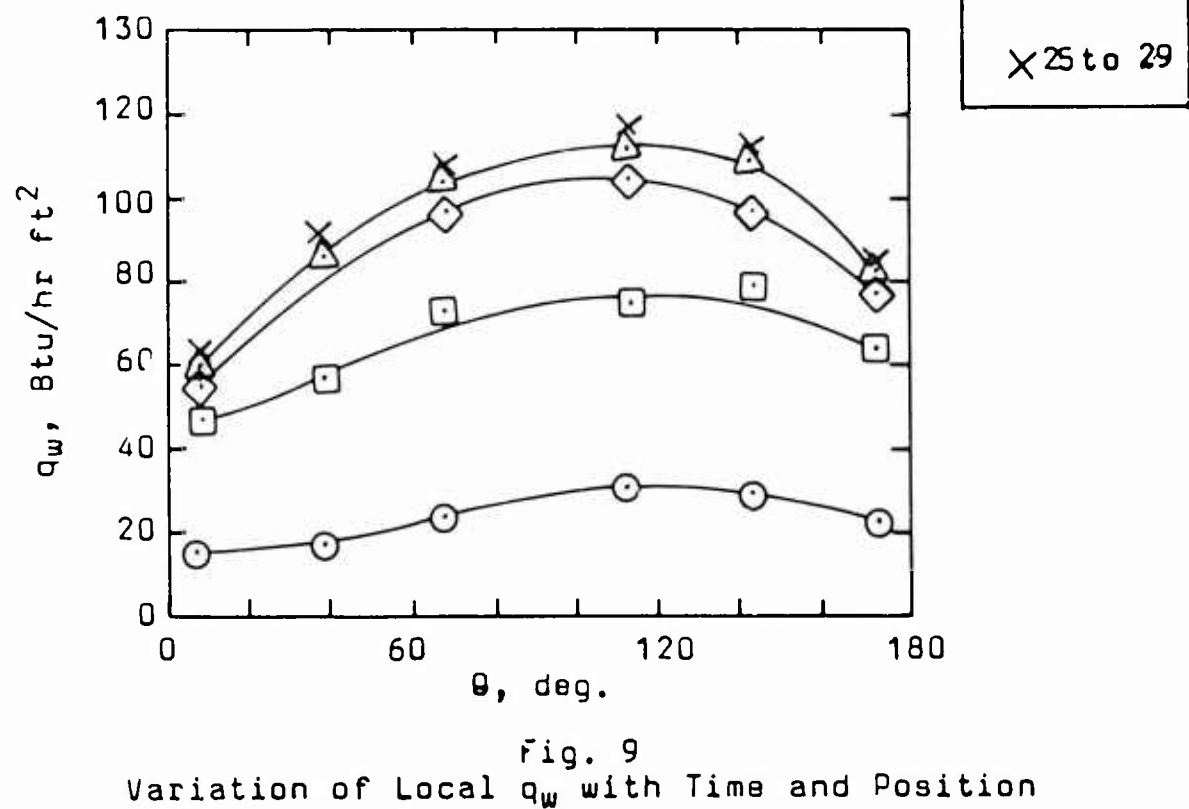
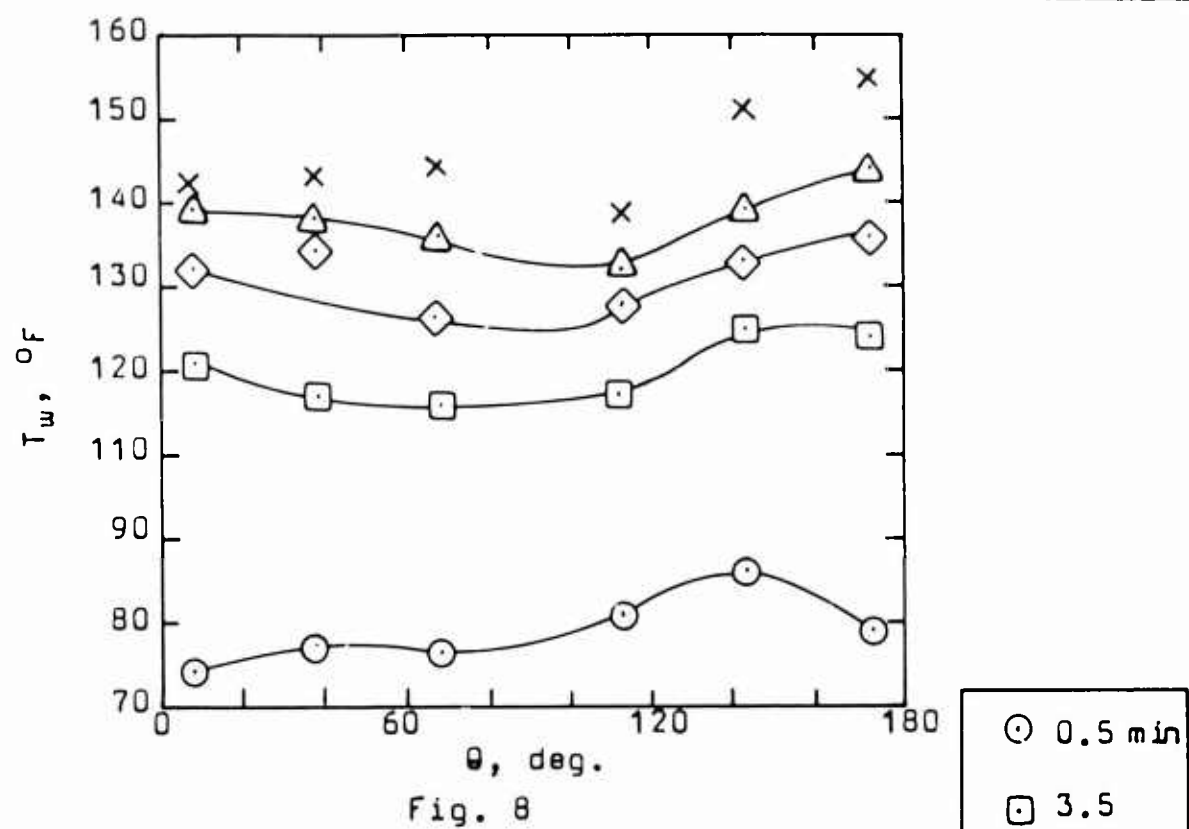
$$\theta = 67\frac{1}{2}^{\circ}$$

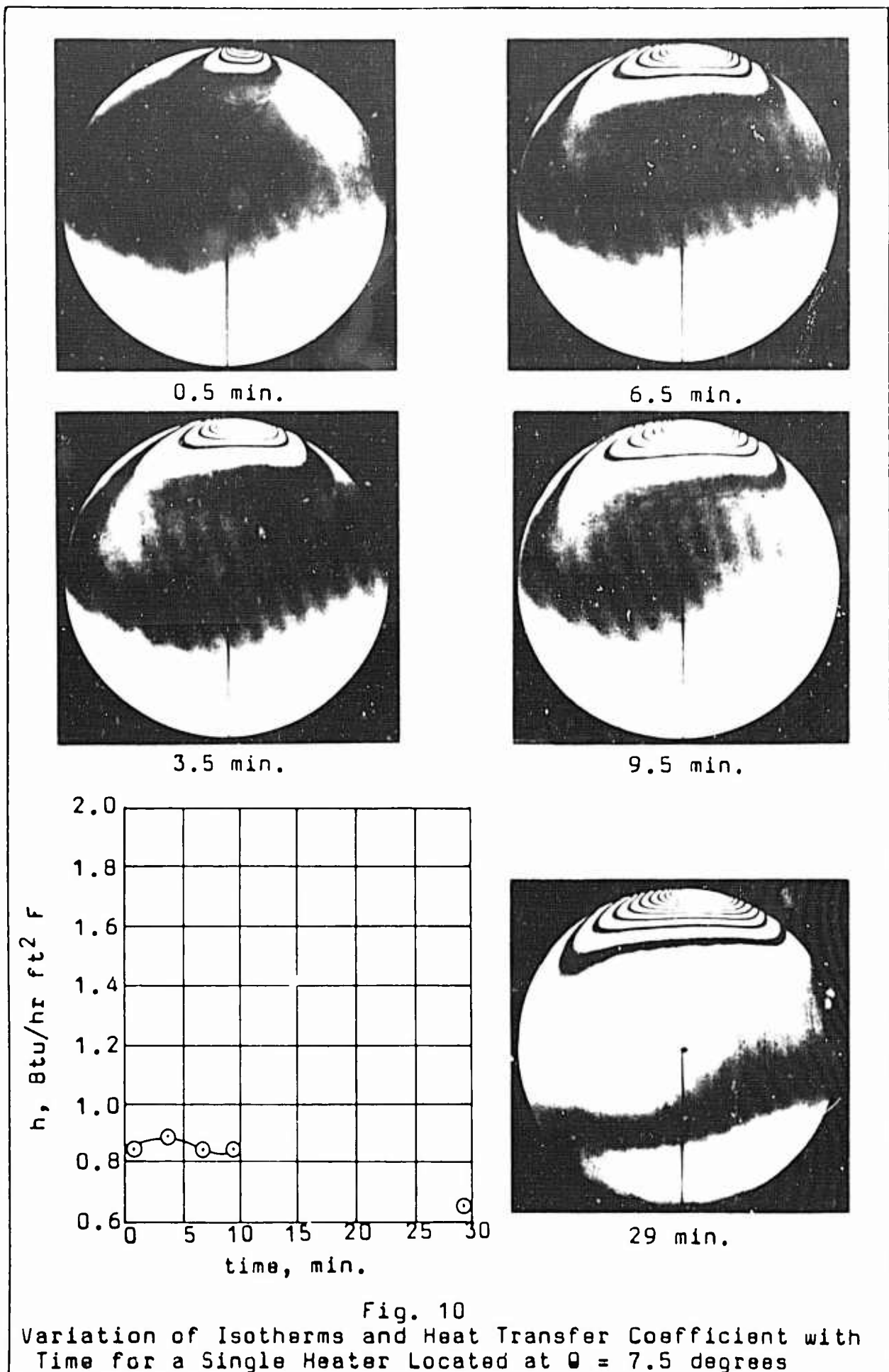


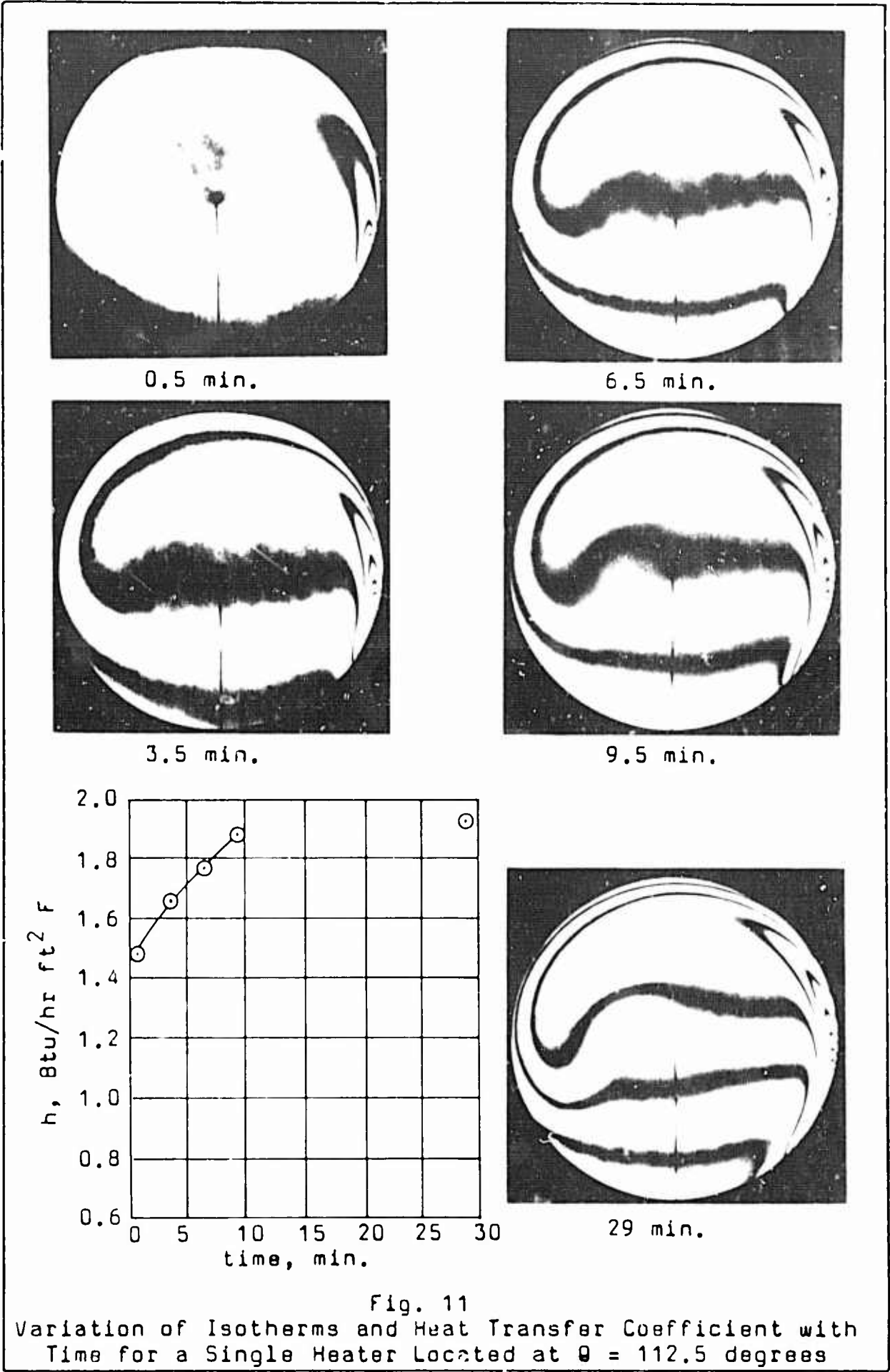
$$\theta = 172\frac{1}{2}^{\circ}$$

Fig. 6  
Isotherm Patterns for Various Heater Locations  
after Five Minutes of Heating









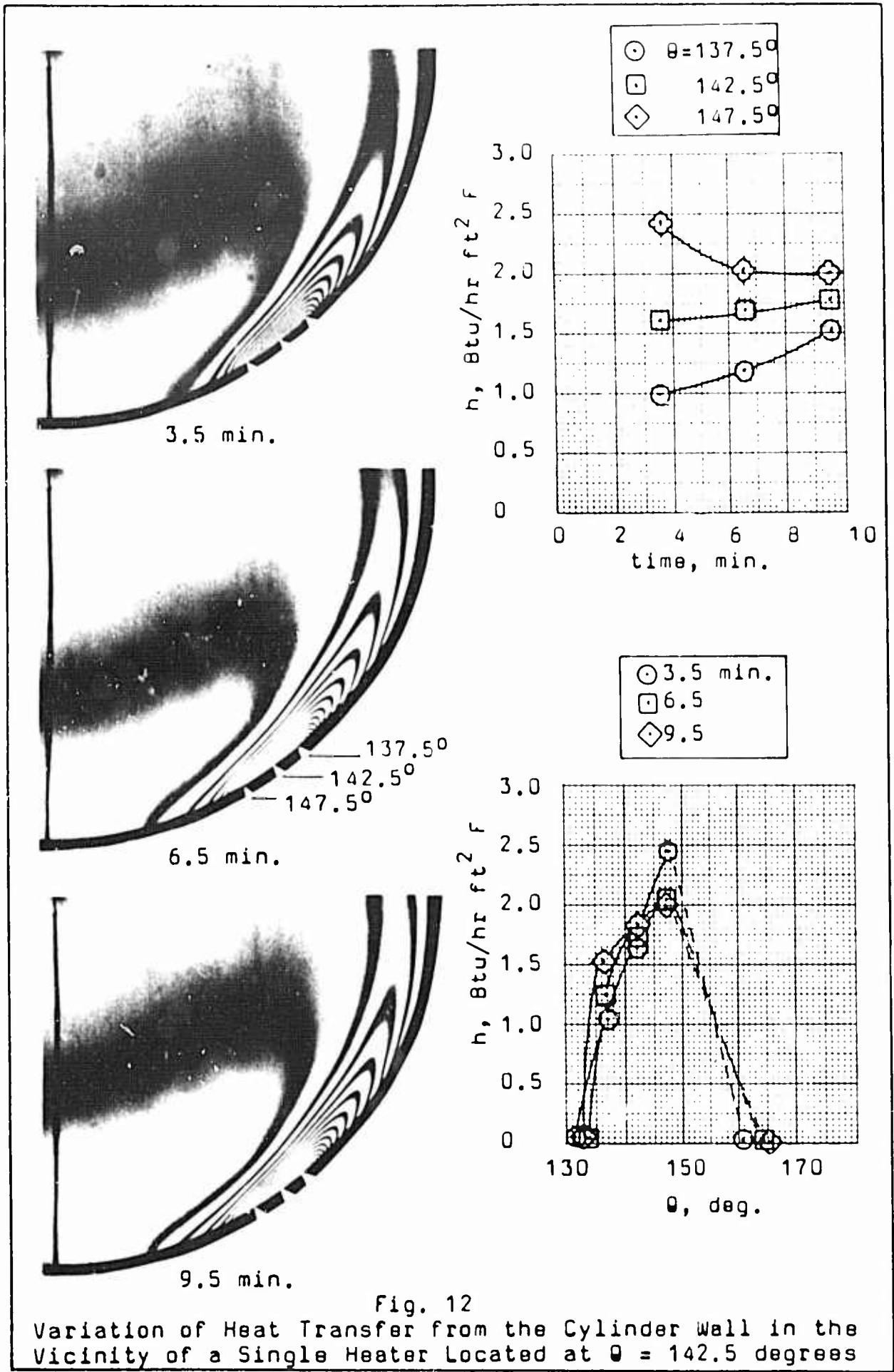


Fig. 12

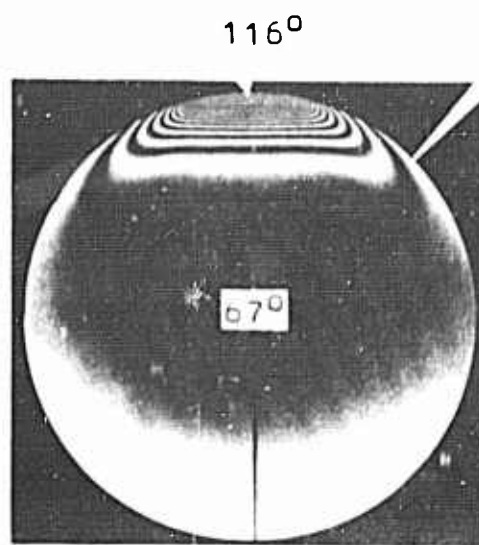
Variation of Heat Transfer from the Cylinder Wall in the Vicinity of a Single Heater Located at  $\theta = 142.5$  degrees



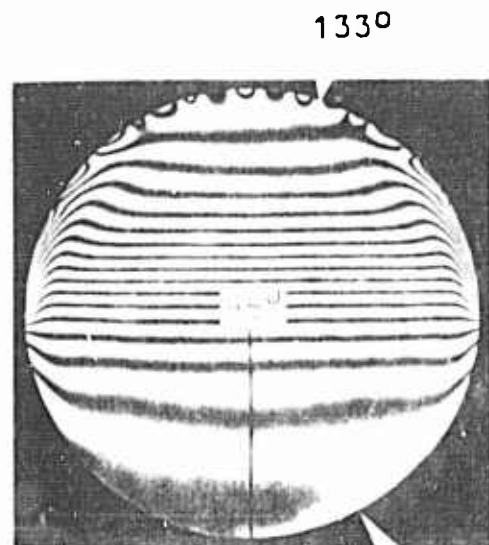
Multiple-heater Configurations

The interferograms presented in Figures 13 and 14 show the isotherm patterns after five minutes of heating for various heater combinations.

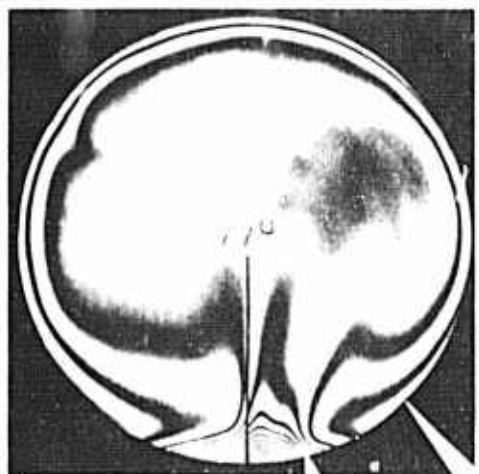
The reference temperature and the maximum and minimum wall temperatures are marked on each photograph. The wall temperature was not measured at the lowest point in the cavity because of the presence of pressure-venting holes.



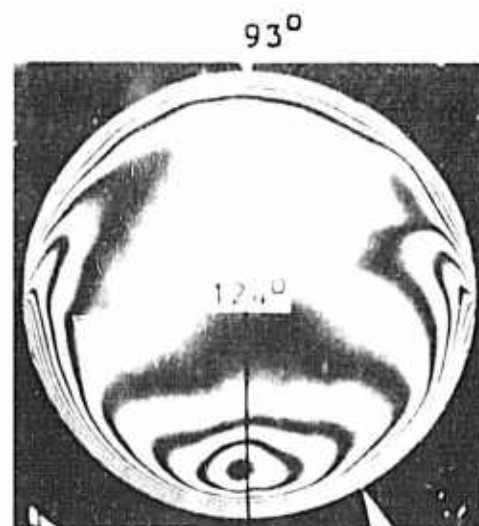
a. Two heaters at top of cylinder



b. Top half of cylinder heated

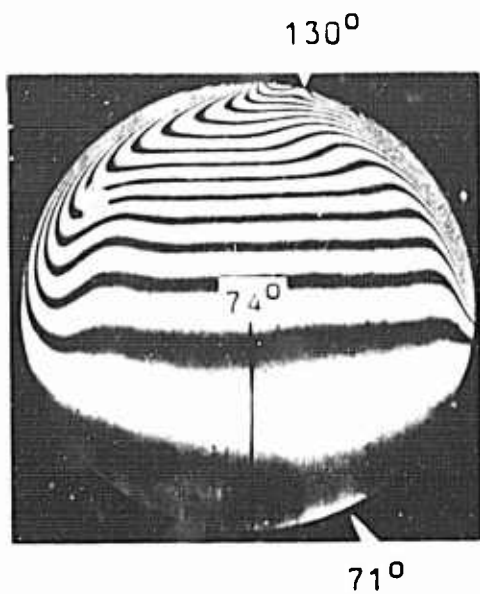


c. Two heaters at bottom of cylinder



d. Bottom half of cylinder heated

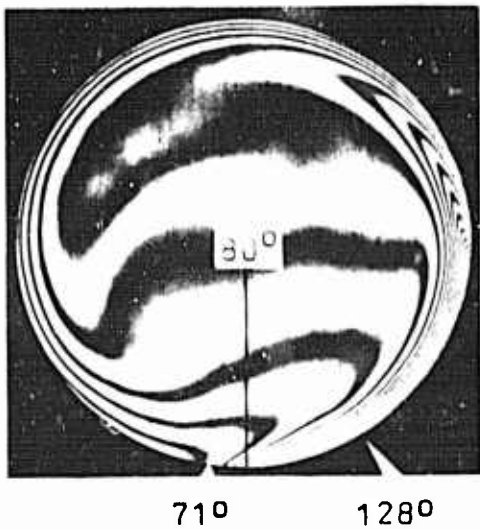
Fig. 13  
Isotherm Patterns for Multiple-Heater Configurations  
after Five Minutes of Heating



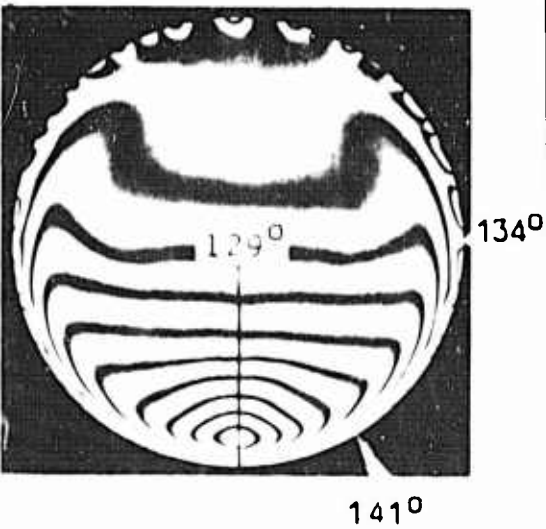
a. Rt. upper quarter heated



b. Rt. half of cylinder heated



c. Rt. lower quarter heated



d. All of cylinder heated

Fig. 14  
Isotherm Patterns for Multiple-Heater Configurations  
after Five Minutes of Heating

## V. Discussion of Results

### Single-Heater Configurations

The isothermal patterns in Fig. 6 illustrate how the buoyant forces, produced when the air is heated, result in the establishment of convective currents in the fluid within the cavity. It is observed that the thermal boundary layer produced by a single heater generally clings to the sides of the cavity and becomes thicker in an upward direction along the heated wall. The thermal boundary layer is noted to be thickest at the top of the cavity and thinnest near the vertical portion of the wall.

In Fig. 7 it may be seen that for the single-heater configurations tested, the local heat transfer coefficient at the wall at each heater has a minimum value at the top of the cylinder and a maximum value near the point where  $\theta = 112.5^\circ$ . This minimum value of  $h$  occurs where the buoyant force is almost directly opposed by the normal wall force. This results in little fluid motion and the formation of a relatively thick boundary layer. At the point where  $\theta = 112.5^\circ$ , the buoyant force which moves the heated air away from the heating surface encounters little opposition from the wall forces. Also the replacement of the rising air by cooler air from below is most efficiently accomplished at this position.

The variation of  $h$  with time may also be observed in Fig. 7. For all values of  $\theta$  except  $112.5^\circ$ ,  $h$  increased initially and then decreased after approximately six

minutes; at the  $112.5^{\circ}$  position  $h$  continued to increase.

Plots of  $q_w$  and  $T_w$  versus time and position are presented in Fig. 8 and 9. Analysis of these curves also indicates that the heat transfer rate is greatest just below the vertical portion of the cylinder wall, and that the most change with time occurs during the first six minutes of heating.

Fig. 12 contains three enlarged pictures of the isothermal patterns at various times for the  $142.5^{\circ}$  heater position. This figure shows how rapidly  $h$  varies with  $\theta$  in the vicinity of a single heater. It also shows that as time of heating increases the individual isotherms near the heater change significantly in size and shape resulting in a corresponding variance in  $h$ .

For 5 of the single heater configurations, the reference temperature in the center of the cavity increased slowly with time with a maximum rate of increase of  $3^{\circ}$  after 9.5 min., and  $8^{\circ}$  after 29 minutes of heating. For the heater located at  $\theta = 172.5^{\circ}$  the temperature increased  $10^{\circ}$  during a 25 min. period with a  $5^{\circ}$  increase occurring in the first 3.5 minutes. This latter behavior is believed to be caused by the near vertical ascent of hot air from this heater as shown by the development of the boundary layer in the interferograms.

#### Multiple-Heater Configurations

The configurations where more than one heating element was used at the same time are shown in Fig. 13 and 14. It

may be observed that when the cylinder is symmetrically heated at the top, no natural convection currents occur in the fluid because the buoyant forces directly oppose the normal wall forces. In this case heat is transported downward by conduction only (neglecting radiation), and the temperature in the fluid is constant in horizontal layers.

The situation is much different when two heaters at the bottom of the cylinder are used. Here, the heated air flows in an upward direction producing an unstable situation, as indicated in Fig. 13c. This behavior is similar to that found in horizontal flat plates when the lower plate is heated (Ref 1:328).

Heating the bottom half of the cavity resulted in the formation of fringes at the top very similar to those formed at the bottom except that the heat was being transferred from the fluid to the wall. The interferogram also shows that a cell containing the coolest air in the cylinder is located near the bottom of the cylinder where the isotherms form relatively small closed loops. This seemed to be caused by a symmetrical circulation of hot air up the sides and down in the center while the cold air moved toward the bottom of the cylinder. This circulation pattern eliminated the turbulence apparent when only two heaters at the bottom were used.

Heating a quarter of the cylinder caused a general thickening of the thermal boundary layer, upward along

the heated wall and downward along the cooler wall. This same behavior resulted when a side half of the cylinder was heated.

Heating the entire cylinder produced a result similar to that shown when just the bottom half was heated and included a lens-shaped core of cold air near the lowest part of the cavity. In addition, horizontal isotherms formed in the lower half of the cylinder and a relatively large constant temperature region formed at the top.

Reference temperatures, shown in Fig. 13 and 14, were read to the nearest degree and were considered to be accurate within  $\pm 0.5^\circ$ . Wall temperatures were measured to an accuracy of  $\pm 0.5^\circ$  at low temperatures and  $\pm 2^\circ$  at  $160^\circ$  F.

## VI. Conclusions and Recommendations

### Conclusions

1. When either the lower half or the entire cylinder wall was heated, the coolest air was located just above the thermal boundary layer at the bottom of the cylinder.

2. When single heaters are used separately, the local heat transfer coefficient at the cylinder wall adjacent to each heater:

- a. had a maximum value in the region 20 to 25 degrees below where the surface is vertical.
- b. increased for approximately six minutes of heating and then decreased. The only exception to this occurred for the heater just below where the wall is vertical, where no decrease with time was noted.

3. An optical interferometer can be used with good results to study natural convection inside a horizontal cavity.

### Recommendations

1. Continue this investigation to:
  - a. define in more detail the mechanism responsible for conclusion 1 and 2.
  - b. include cylinder diameter and gases other than air as additional parameters.
  - c. relate cylindrical heat transfer data to



GAM 65A/ME/65-3

that of a vertical flat plate.

2. Embed thermocouples in the fiberglass to increase the accuracy of temperature measurements.

Bibliography

1. Eckert, E. R. G. and Drake, R. M., Heat and Mass Transfer. New York: McGraw-Hill Book Company, Inc., 1959.
2. Eckert, E. R. G. and Soehngen, E. E., Studies on Heat Transfer in Laminar Free Convection with the Zehnder-Mach Interferometer. AFTR 5747. Wright-Patterson Air Force Base, Ohio: Wright Air Development Center, 1948.
3. Rich, B. R., "An Investigation of Heat Transfer From an Inclined Flat Plate in Free Convection." Transactions of the American Society of Mechanical Engineers, 75: 489-499, 1953.

Contents

	Page
Appendix A: Single-heater Interferograms . . . .	29
Appendix B: Details of Apparatus and Dis- cussion of Errors . . . . .	34
Appendix C: Sample Calculations . . . . .	39
Appendix D: Tabulated Data . . . . .	41
Vita . . . . .	42

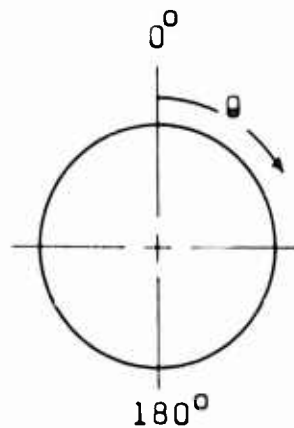
List of Figures

Figure		Page
15	Variation of Isotherms and Heat Transfer Coefficient with Time for a Single Heater Located at $\theta = 37.5$ degrees . .	30
16	Variation of Isotherms and Heat Transfer Coefficient with Time for a Single Heater Located at $\theta = 67.5$ degrees . .	31
17	Variation of Isotherms and Heat Transfer Coefficient with Time for a Single Heater Located at $\theta = 142.5$ degrees. .	32
18	Variation of Isotherms and Heat Transfer Coefficient with Time for a Single Heater Located at $\theta = 172.5$ degrees. .	33
19	Experimental Apparatus . . . . .	34
20	Sketch of Typical Cylinder Wall Section	35
21	Heating Equipment . . . . .	37

Appendix A

Interferograms of Single—heater Configurations

A curve of  $h$  versus time for each configuration is included with the photographs which were used to evaluate the data points. A composite plot of these curves is presented in Fig. 7.

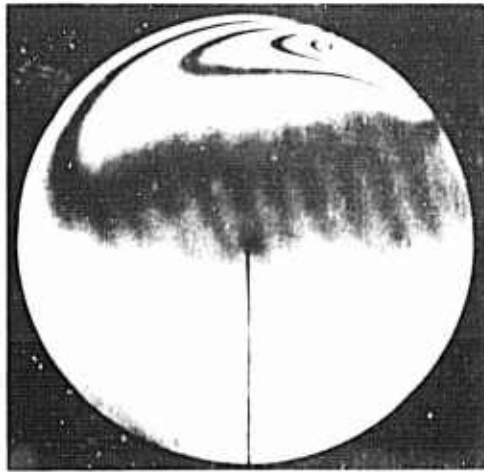




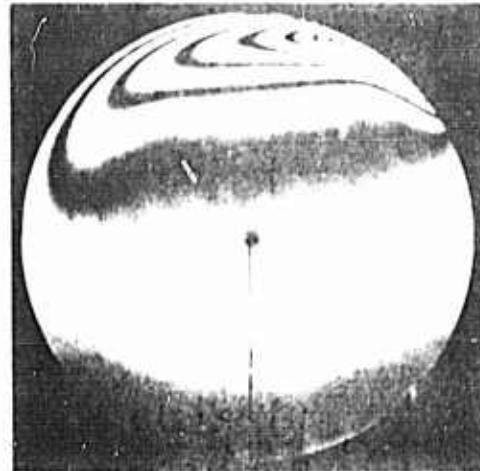
0.5 min.



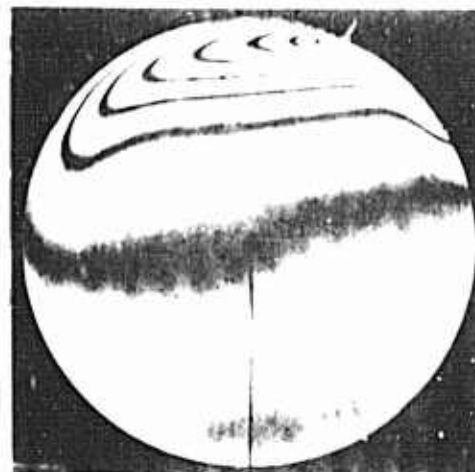
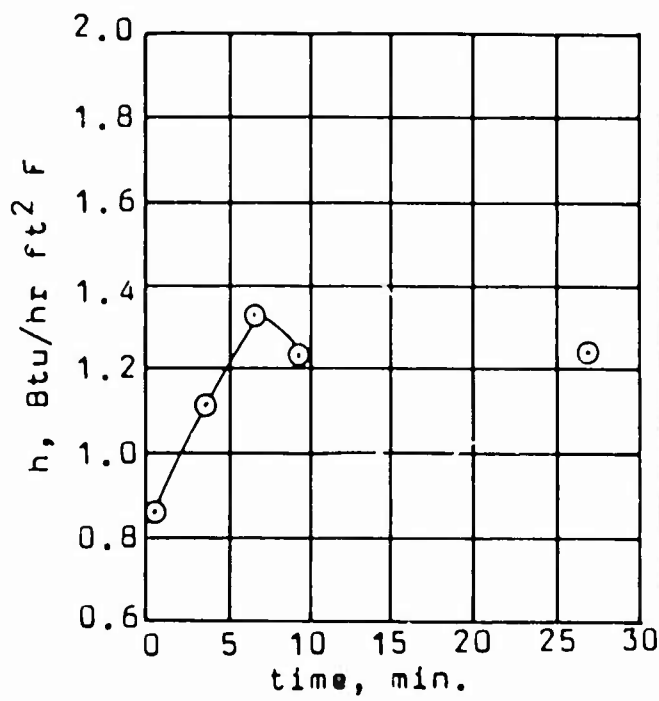
6.5 min.



3.5 min.

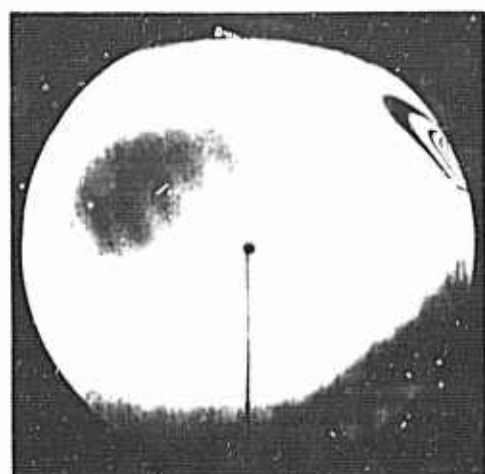


9.5 min.



27 min.

Fig. 15  
Variation of Isotherms and Heat Transfer Coefficient with Time for a Single Heater Located at  $\theta = 37.5$  degrees



0.5 min.



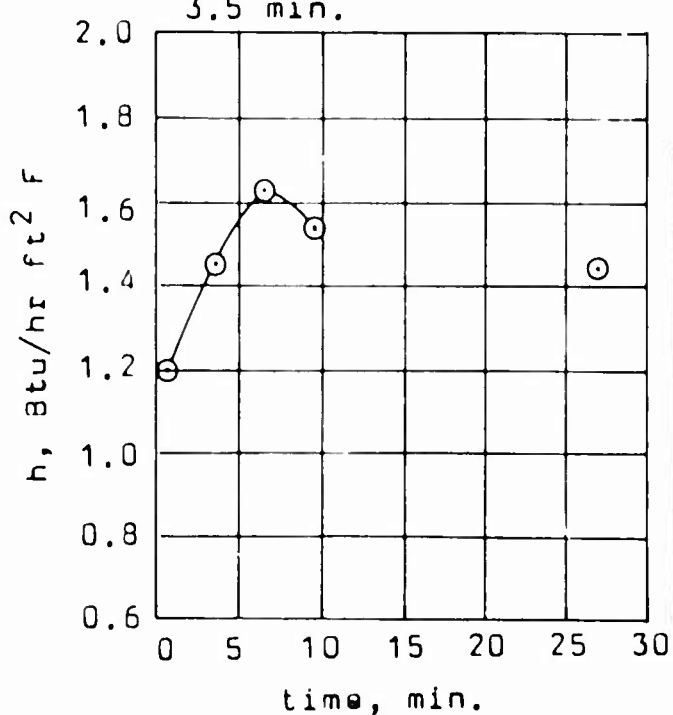
6.5 min.



3.5 min.

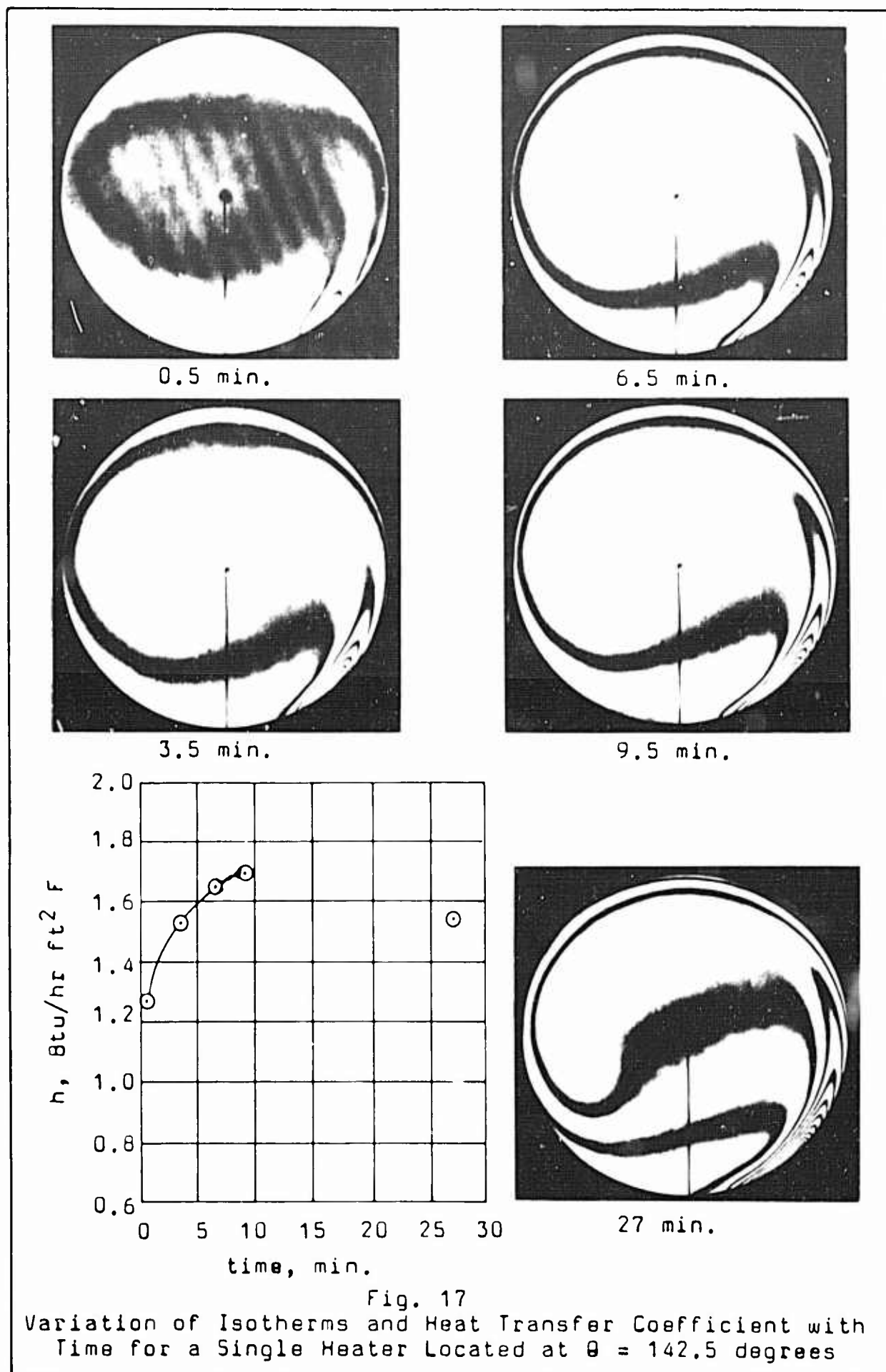


9.5 min.



27 min.

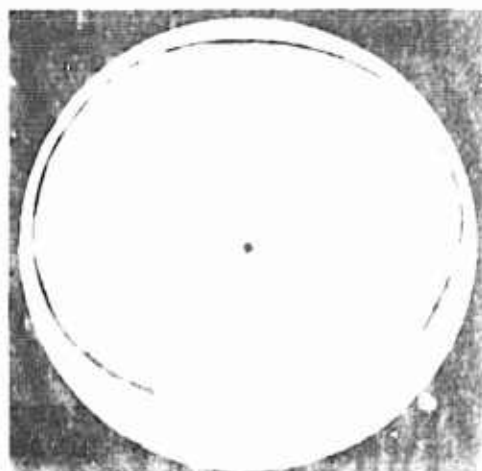
Fig. 16  
Variation of Isotherms and heat Transfer Coefficient with  
Time for a Single Heater Located at  $\theta = 67.5$  degrees







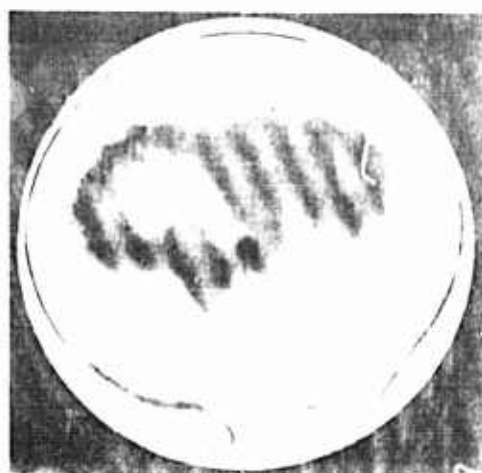
0.5 min.



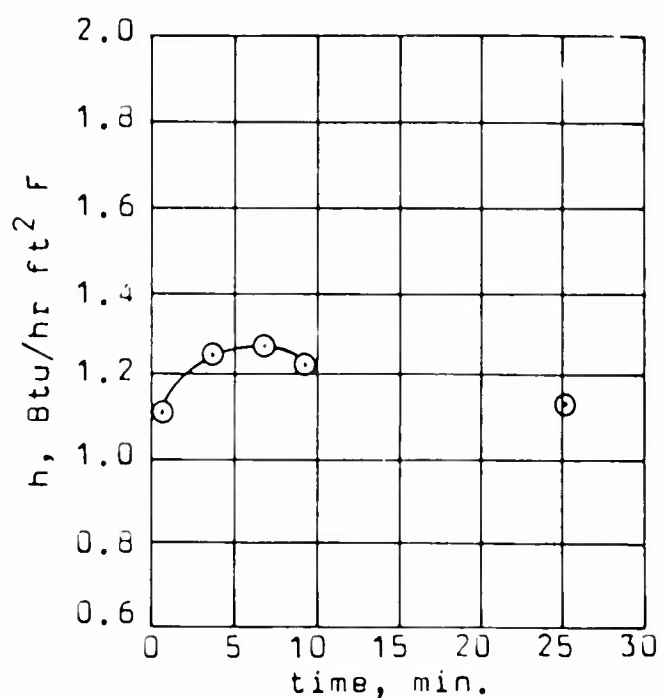
6.5 min.



3.5 min.



9.5 min.

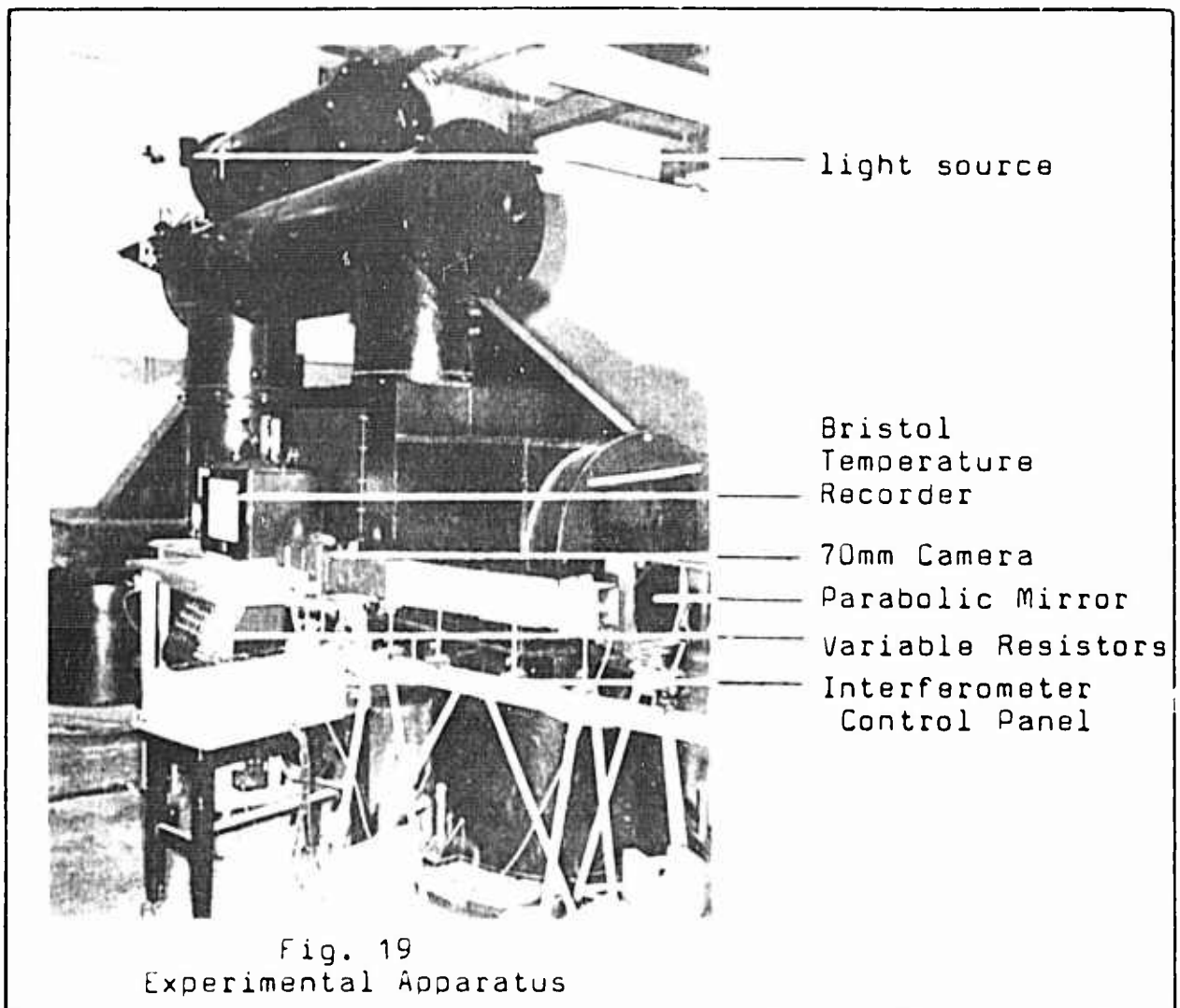


25 min.

Fig. 18  
Variation of Isotherms and Heat Transfer Coefficient with Time for a Single Heater Located at  $\theta = 172.5$  degrees

Appendix B

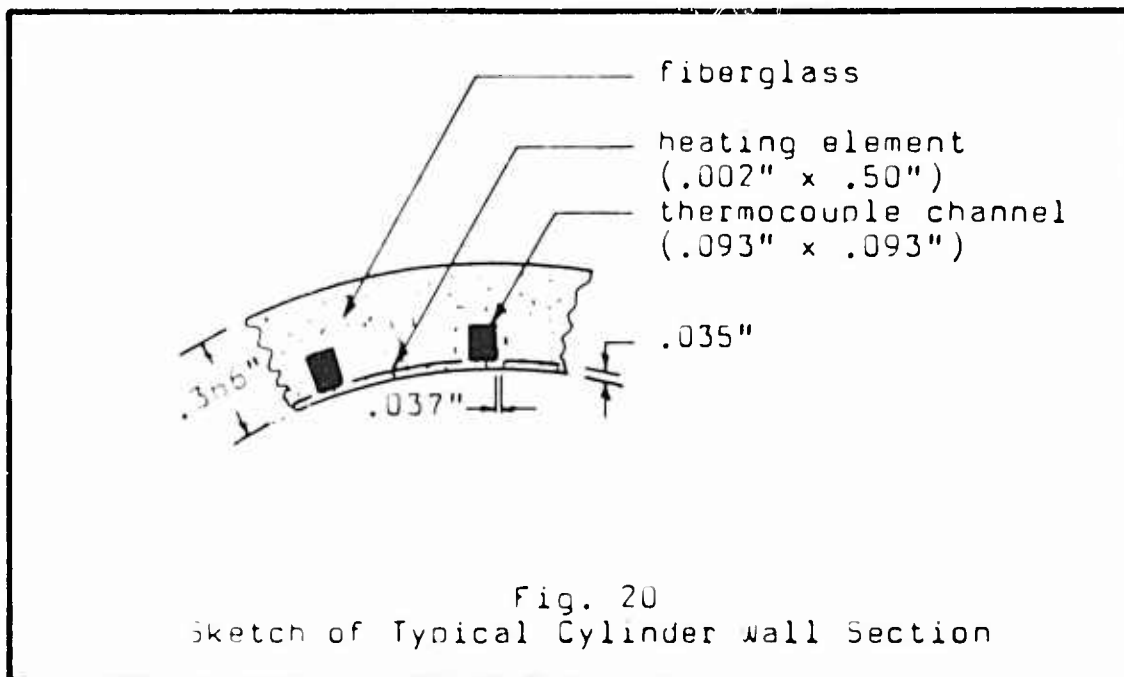
Details of Apparatus



The photograph of the experimental apparatus, Fig. 19, shows some of the apparatus explained in Chapter II.

The fiberglass cylinder was manufactured by the AFIT School Shops. A stainless steel mandrel, ground with a five-thousandths taper, was used to form the

cylinder. A polyester resin\* was used with two types of glass cloth. The inner 0.010 in. of the cylinder was built up using a continuous 12-in. wide piece of glass cloth which weighed 2 oz/yd and was 0.003 in. thick. The remaining portion of the cylinder was made of a continuous strip of 1-in. wide cloth which weighed 7½ oz/yd and was 0.010 in. thick. This cloth was wrapped with a 0.5 in. overlap and a special technique using mylar tape was applied to eliminate air bubbles in the resin during the manufacture of the cylinder. Grooves were milled into the cylinder to permit accurate placement of the heating ribbons and of the square drill rods which were used to make cavities for the sliding thermocouples.



\* AR-28C Polyester Resin  
Celanese Corp. of America  
Plastics Division  
744 Broad St., Newark, N. J.

The fiberglass test cylinder had heating elements embedded in it parallel to the longitudinal axis of the cylinder. Heating element dimensions were 0.50 in. wide, 0.002 in. thick, and 12.0 in. long. Iron-constantan thermocouples (30-gauge) were placed in the small cavities between each of the 24 heating elements. Both ends of the cavities were sealed with epoxy resin. The welded thermocouple junctions were positioned six inches from either end of the cylinder and were forced against the inside wall of each cavity by strips of balsa wood. Cardboard tubes, not shown in the photographs, were placed between the glass end plates and the interferometer to isolate the light beam from air currents in the room. Constant pressure conditions within the test subject were maintained by drilling twenty-three 1/32-in. diameter holes from the interior of the cylinder into the thermocouple channel located at the bottom of the cylinder. This channel was then vented to the atmosphere.

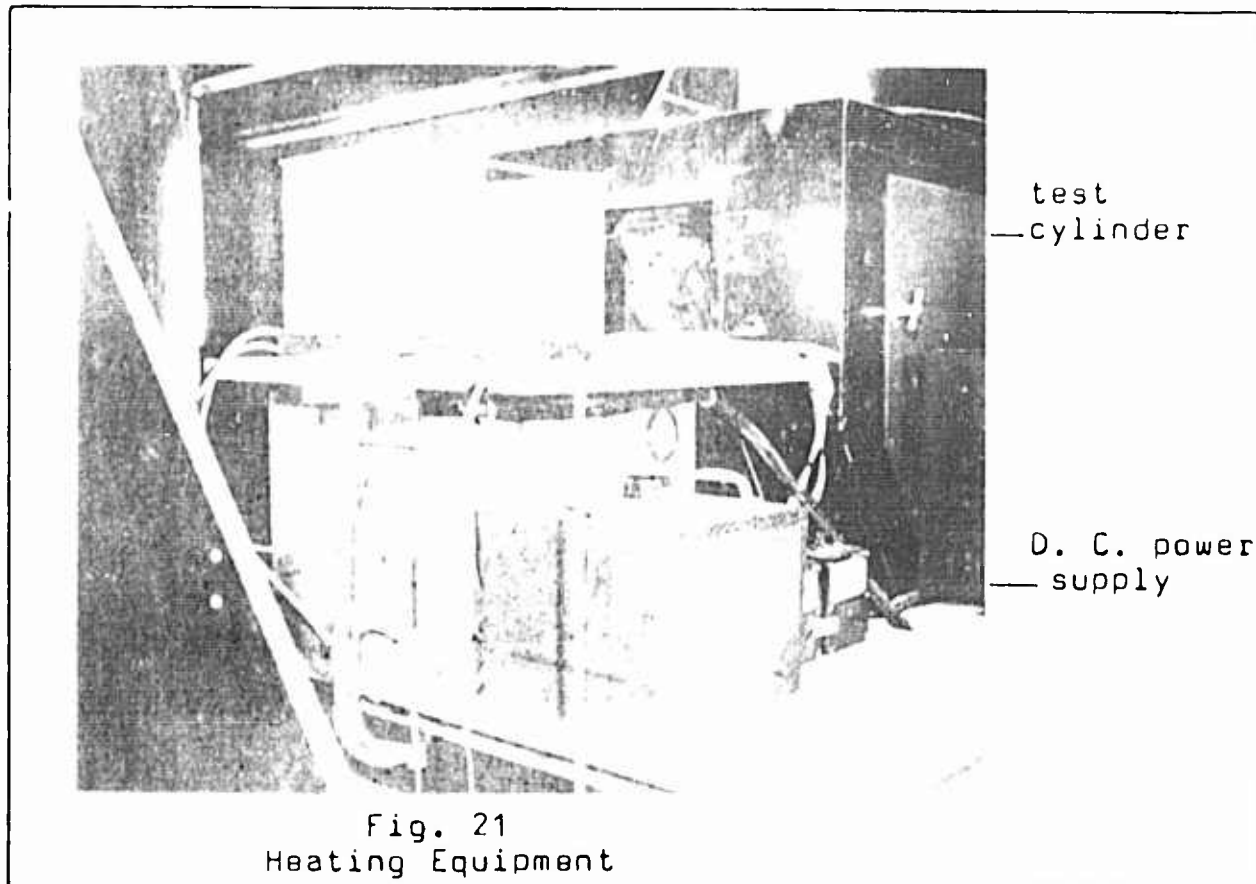


Fig. 21 shows the test cylinder and the equipment which was used to heat the cylinder and measure the voltage and current input. The heating elements were Nichrome (Alloy V) high-resistance ribbon made by the Driver-Harris Company, Harrison, New Jersey. This alloy, 80% nickel and 20% chromium, has a rated resistance of 0.496 ohms per foot, and has a linear variation of resistance over the temperature range encountered in this experiment. Copper terminal plates were soldered to each end of the heater elements.

The electrically operated 70mm camera was connected to an intervalometer which provided the electric triggering pulses at a selected rate. The camera lens was replaced by a parabolic mirror with a focal length of 7.5 ft.

### Discussion of Errors

Errors, considered to be negligible in this study, include those caused by the interferometer; the cylinder construction, alignment, and end effects; temperature measurements; and evaluation techniques. The most significant interferometer error was caused by the bending of light rays when they passed through non-homogeneous density fields. Light rays entering the test section in an area of high density gradient, normal to a heated surface, bend away from or toward the surface depending on the direction of the gradient. The main error produced by the cylinder construction resulted from the fact that it was necessary to include a 0.005-inch taper over the length of the cylinder so that it could be removed from the steel mandrel. The cylinder was placed with the smallest end nearest the light source so that the increasing diameter tended to compensate for the previously mentioned bending of the light rays, and for this reason both effects were neglected. Errors caused by misalignment of the glass end-plates were considered to be insignificant even though this was the probable cause of a faint second image visible in some of the photographs.

All interfurograms showed the cylinder to be flattened slightly. This was the result of deflecting the light beam off the centerline of the parabolic mirror for viewing purposes.

## Appendix C

Sample Calculations

The local heat transfer coefficients contained in this report were evaluated in the manner explained below.

A sample calculation is shown for a single heater at  $\theta = 7.5^\circ$ , after 9.5 minutes of heating. The photograph corresponding to this condition is shown in Fig. 10. Calculations for density and temperature differences between fringes were made with a slide rule. The atmospheric pressure for this run was 29.53 inches of mercury or  $2090 \text{ lb/ft}^2$  and the reference temperature was 529R. Using the ideal gas law:

$$\rho_r = \frac{p}{RT}$$

$$\rho_r = \frac{2090 \text{ lb/ft}^2}{53.3 \frac{\text{ft} \cdot \text{lb}}{\text{lb} \cdot \text{R}} 529\text{R}}$$

$$\rho_r = 0.0741 \text{ lb/ft}^3$$

with equation (1) presented in Chapter III,

where  $\frac{\rho_r}{\rho_{\infty}} = 5.1 \times 10^{-4} \text{ lb/ft}^2$  for air as the gas and  $\lambda_0 = 5461 \text{ Å}$  as in the filtered mercury lamp (from page 188 of Aerodynamic Measurements, M.I.T., 1953, by R. C. Dean, Jr.).

$$L = 1.00 \text{ ft cylinder length}$$

$$\rho_0 = 0.0741 - 0.00051r$$

Evaluating the 5th fringe in from the center of the cylinder

$$\rho_5 = 0.0741 - 0.00051 (5)$$

$$\rho_5 = 0.0715 \text{ lb/ft}^3$$

$$T_5 = \frac{P}{\rho_5 R} = \frac{2090}{53.3 (0.0715)}$$

$$T_5 = 548^{\circ} \text{ R}$$

After evaluating the temperature at each fringe, a 38 mm Gaertner Comparator was used to measure the fringe spacing from the photograph, and a plot of  $T_e$  vs  $r$  was made. The temperature gradient at the wall and the wall temperature were obtained directly from the plot. Then  $h$  was evaluated using equation (5) in Chapter III.

$$h = \frac{-k_w (dT/dr)_w}{(T_w - T_r)}$$

$$h = \frac{-0.0166 (-3590)}{(599 - 529)}$$

$$h = 0.85 \text{ BTU/hr ft}^2 ^{\circ}\text{R}$$





VITA

Captain Richard I. Erb was born

\_\_\_\_\_, \_\_\_\_\_, \_\_\_\_\_, \_\_\_\_\_, \_\_\_\_\_ PII Redacted

After completing two years of college at Pasadena City College, he enlisted in the USAF. He graduated from pilot training and was commissioned in March 1953. Following a tour of duty as an F-89 interceptor pilot at Elmendorf AFB, Alaska, he was assigned to the University of Washington from which he graduated with a Bachelor of Science degree. Before coming to the Air Force Institute of Technology, he worked as an aeronautical research engineer in the Flight Dynamics Laboratory at Wright-Patterson AFB, Ohio.

Permanent address:

\_\_\_\_\_

PII Redacted